

# Estimation of Parameters of a Snow Cover on a Ground Surface without a Relief and with Relief by the Radar Interferometry Method

Pavel .N.Dagurov<sup>1,2</sup>, Aleksey V. Dmitriev<sup>1</sup>, Sergey I. Dobrynin<sup>2</sup>, Tumen N. Chimitdorzhiev<sup>1</sup>

<sup>1</sup> Institute of Physical Materials Science of SB RAS, Ulan-Ude, Russia, pdagurov@gmail.com

<sup>2</sup> Buryat State University, Ulan-Ude, Russia, pdagurov@gmail.com

<sup>3</sup> Buryat Institute of Infocommunications of SibSUTIS, Ulan-Ude, Russia, wmdumb@gmail.com

**Abstract.** The remote sensing of snow cover is studied using radar interferometry. An approximate model of interferometric sounding based on the small perturbation method is proposed. The contribution of the scattering from the snow surface to the amplitude and interferometric phase was estimated. The analysis of the effect of the relief on the assessment of snow cover parameters was performed. The results of numerical estimates are given.

**Keywords:** snow water equivalent; radar interferometry; small perturbation method; relief.

## 1 Introduction

Seasonal snow cover in the regions of temperate and northern latitudes is an important natural factor. Snow has a great impact on climate, hydrological and soil processes, plant and animal life, and human life.

The main characteristics of the snow cover that determine its impact on the environment are its thickness and the snow water equivalent (SWE) [1]. The snow water equivalent determines the water content in the snow cover. In particular, in the case of homogeneous snow with a constant height, the snow water equivalent is defined as the product of the depth of snow cover  $d$  and its density  $\rho_s$ , referred to the density of water  $\rho_w$ , and is expressed in units of length.

Using the method of radar interferometry has shown that it is an effective tool for the diagnosis and monitoring of various changes in the earth's cover [3 - 6]. Interferometric methods were also used to analyze the snow cover and estimate the snow water equivalent [7 - 11]. The possibility of direct measurements of SWE using differential interferometry was first considered in [7]. In [8], the results of experiments in the C-band using the remote sensing satellites ERS-1 and ERS-2 are presented, which show agreement with the calculated dependences. The theoretical dependence for the interferometric phase on the wind farm was also used in [8] for comparison with experimental data obtained from span SAR flights in the L-band. A comparison of the calculation formula for determining SWE of dry snow and experimental results was carried out in [9]. In [10], Sentinel-1 radar data were used to estimate the wind farm. In [11], similar estimates were performed by analyzing the ALOS PALSAR 2 data obtained at a test site on the shores of Lake Baikal.

Earlier in [12], a model of backscattering from snow cover on a flat average Earth's surface was proposed. Backscattering occurs due to small-scale roughness. In this paper, we present some numerical results for this situation and consider the more general case of scattering from snow cover on a surface with a relief..

## 2 Backscattering from snowpack without relief

When constructing a model for the backscattering of microwaves from a dry snowpack on the soil, we assume that snow is a continuous homogeneous medium and that there is no volumetric scattering. This is true in the C- and especially in the L-bands when the size of the snow particles is much smaller than a wavelength. Figure 1 shows the geometry of the problem and the paths of microwaves along which they propagate in the absence and presence of a snowpack. In the absence of snow, the wave designated as 1, falling from the air onto the soil at an angle of  $\theta_i$ , is scattered back by the roughness of the soil in the form of the  $w_{ag}$  wave (red dashed line). Note that Figure 1 shows trajectories of the incident waves by solid lines and those of the scattered waves using dashed ones. In the presence of a snowpack, when wave 2 falls onto the snowpack from the air at an angle of  $\theta_i$ , it refracts and propagates in the snow

layer. Afterward, wave 2 falls onto the “snow–ground” interface at an angle of  $\theta_i$ , and the same roughness of the soil scatters the wave back as the  $w_{sg}$  wave (green dashed line). The single-wave model of Guneriusen et. al. [30] takes into account only this scattered wave. Let us consider a more general model that takes into account the backscattering wave from the “air–snow” interface. Assume that radar wave 2 falls from the air at the angle  $\theta_i$  onto the snow layer covering the ground (Figure 1). The radar is in the far zone and the incident wave can be considered as a plane wave  $\vec{E}_p = \vec{E}_{0p} e^{jk(x \sin \theta_i - z \cos \theta_i)}$  ( $k$  is a wavenumber in the air). Here and below, the  $p$  index describes the polarization of the radiation:  $p = h$  when the polarization of the radiation is horizontal and  $p = v$  for vertical polarization.

Copyright © by the paper’s authors. Copying permitted for private and academic purposes.

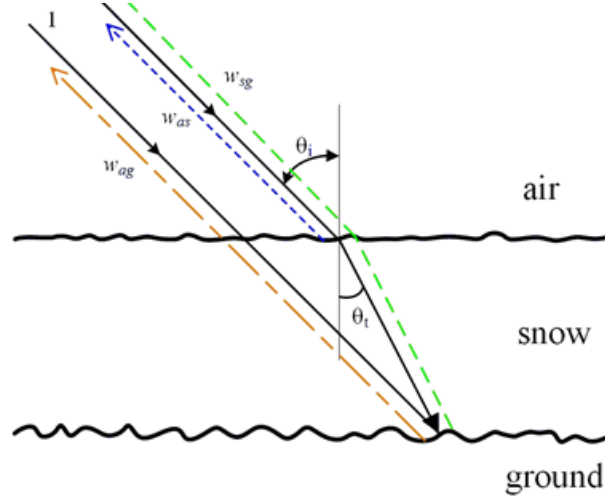


**Figure 1.** Geometry of backscattering from soil in the absence and presence of a snowpack.

Homogeneous ground is characterized by a complex dielectric constant  $\varepsilon_g = \varepsilon'_g + j\varepsilon''_g$ ; dry snow is assumed to be a non-absorbing medium with a dielectric constant  $\varepsilon_s$ , and the dielectric constant of air is equal to 1. The boundary surfaces of “air–snow” and “snow–soil” are statistically rough ones with random irregularities. Their heights are uncorrelated with each other and described by stationary random functions  $z_s(x, y)$  and  $z_g(x, y)$ , with mean values equal  $\langle z_s \rangle = d$  and  $\langle z_g \rangle = 0$  (where  $d$  is the average depth of the snowpack), standard deviations equal to  $b_s$  and  $b_g$ , and correlation radii of  $l_s$  and  $l_g$ , respectively. If we let irregularities be small compared with the wavelength, then their slopes are insignificant and the small perturbation method (SPM) applicability conditions, such as  $kb_s, kb_g < 0,3$  and  $kl_s, kl_g < 3$  [13], are satisfied. It is assumed that irregularities do not influence the coherent field (Born approximation). The incident wave passes through the snow layer at the angle  $\theta_i$ , determined by the Snell–Descartes law. When leaving the snow, the scattered wave also refracts according to the Snell–Descartes law. Fresnel formulas for a flat interface are used to calculate the reflection and transmission coefficients of coherent waves. The backscattered field is the coherent sum of the waves scattered by the irregularities of boundaries. The first wave is the  $w_{as}$  wave scattered by the “air–snow” interface (blue dashed line in Figure 1), and second one is the  $w_{sg}$  wave backscattered by the “snow–ground” interface that occurs after the wave passes through the layer and emerges from it (main scattered wave). In addition to these waves, weaker backscattering waves appear because of reflections from the layer interfaces and scattering by irregularities. However, we can neglect the influence of these waves because the values of the reflection coefficient from the “dry snow–air” interface is insignificant (see the next subsection). We do not take into consideration phase fluctuations of waves caused by small irregularities at media interfaces. Let us suppose that phase values are due to the paths of the waves and their interaction with averaged flat interfaces in the framework of the small perturbation method. Then, a random electromagnetic field with an amplitude  $E_p$  and phase  $\Phi$  backscattered by rough boundaries can be expressed by the following sum:

$$|E_p| e^{j\Phi} = |E_{sp}| e^{j\Phi_s} + T_{sp} T'_{sp} |E_{gp}| e^{j\Phi_g}, \quad (1)$$

where the summands on the right-hand side of the formula describe the  $w_{as}$  and  $w_{sg}$  wave fields, respectively. In (1),  $T_{sp}$  and  $T'_{sp}$  are Fresnel transmission coefficients of the wave that propagates through the averaged flat “air–snow” interface in the forward and backward directions, respectively;  $E_{sp}$  is the amplitude of the field scattered by snow irregularities in Figure 1;  $E_{gp}$  is the amplitude of the field scattered by the uneven ground.  $\Phi_s$  is the interferometric phase of the wave backscattered by snow.  $\Phi_g$  is the interferometric phase of the wave backscattered by the ground after passing through the snowpack in the forward and backward directions

$$\Phi_s = \psi - \varphi_0, \quad \Phi_g = \varphi + \psi - \varphi_0, \quad (2)$$

where  $\varphi = 2k \sqrt{\varepsilon_2} d / \cos \theta_s$ ,  $\psi = 2kd(\operatorname{tg} \theta_i - \operatorname{tg} \theta_t) \sin \theta_i$ ,  $\varphi_0 = 2kd / \cos \theta_i$

After averaging relation (1), we obtain

$$\langle |E_p| \rangle e^{j\Phi} = \langle |E_{sp}| \rangle e^{j\Phi_s} + T_{sp} T'_{sp} \langle |E_{gp}| \rangle e^{j\Phi_g} \quad (3)$$

where the expressions in angled brackets represent the average amplitudes of the scattered fields. We assume that the squares of these average amplitudes are proportional to the mean squares of the amplitudes. This is true, for example, for random values distributed according to the Rayleigh law. Since the mean square of the backscattering field amplitude is proportional to the backscattering coefficient, it follows from expression (3) that

$$\sqrt{\sigma_p^0} e^{j\Phi} = \sqrt{\sigma_{sp}^0} e^{j\Phi_s} + T_{sp} T'_{sp} \sqrt{\sigma_{gp}^0} e^{j\Phi_g} \quad (4)$$

where  $\sigma_p^0$  is the resulting backscattering coefficient,  $\sigma_{sp}^0$  is the backscattering coefficient from the “air–snow” interface, and  $\sigma_{gp}^0$  is the backscattering coefficient from the “snow–ground” interface.

The value  $\sqrt{\sigma_p^0} e^{j\Phi}$  can be called a complex amplitude-backscattering coefficient. Taking into consideration the relations between transmission coefficients and a reflection coefficient  $R_{sp}$  from the “air–snow” interface  $T_{sp} = 1 + R_{sp}$ ,  $T'_{sp} = 1 - R_{sp}$ , we can rewrite equation (4) in the following form:

$$\sqrt{\sigma_p^0} e^{j\Phi} = \sqrt{\sigma_{sp}^0} e^{j\Phi_s} + (1 - R_{sp}^2) \sqrt{\sigma_{gp}^0} e^{j\Phi_g}. \quad (5)$$

Further, for calculations, we will use the known expressions of the backscattering coefficients in the approximation of the small perturbation method [12]. The dielectric constant of dry snow is determined by the expression [14]

$$\varepsilon_s = 1 + 1.6\rho + 1.86\rho^3 \quad (6)$$

where  $\rho$  is the numerical value of the snow density and is expressed in g/cm<sup>3</sup>. This ratio is valid for frequencies in the range from 100 MHz to 10 GHz and for a snow density of less than 0.5 g/cm<sup>3</sup>.

Figure 3 shows the relative interferometric phase  $\delta\Phi = \Delta\Phi/\Phi_g$  variations when the snow depth changes. The presented dependencies show that the variations can exceed 10% in the situations under consideration. Notice that as the depth of snow increases, variations in the relative phase decrease. This result is due to the fact that when the depth of the snow increases, the value of  $\Phi_g$  grows faster than  $\Delta\Phi$ . If the snow depth is greater than 40 cm, then  $\delta\Phi < 4\%$ . This means that in the considered hypothetical case, in which the root-mean-square values and correlation radius of irregularities on the surfaces of the soil and the snow are equal, the impact of backscattering from the “air–snow” interface on the interferometry phase is rather weak.

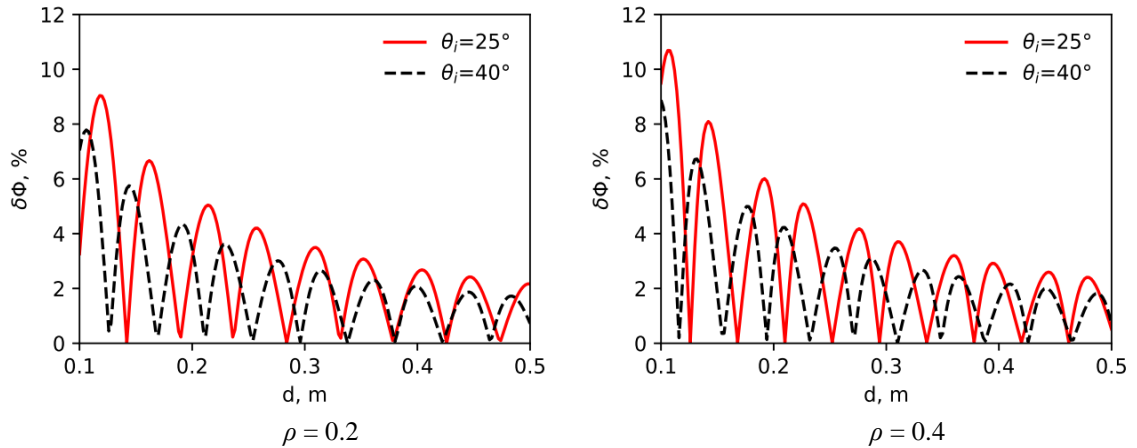


**Figure 2.** The relative interferometric phase variations in the radar signal versus the snow depth.

The phase difference of the main backscattering wave that has passed the snow cover and the backscattering wave in the absence of snow cover is determined according to the relation [7].

$$\Phi_1 = 2kd(\sqrt{\varepsilon_s - \sin^2 \theta_i} - \cos \theta_i). \quad (7)$$

Estimates show that the interferometric phase of the main scattered wave is linearly related to the snow density with good accuracy and, accordingly, it is directly proportional to the WES (SWE). This important result for practice was obtained for the first time in [7]. The relationships between the interferometric phase and the density of snow and wind farm (SWE) are obtained in the form

$$\Phi_1 = 1.5kd\rho/\cos\theta_i \quad SWE = \Phi_1 \cos\theta_i/(1.5k) \quad (8)$$

An estimate of the relative error in determining the interferometric phase due to the influence of a wave scattered by the air – snow boundary and the nonlinearity of formula (7) shows that the resulting error of formula (8) does not exceed 8% for incidence angles of  $20^\circ - 45^\circ$  and snow density  $(0.2 - 0.3) \text{ g/cm}^3$ .

### 3 Assessment of the effect of the relief on the interferometric phase

The above backscattering model from snow cover considers the case of on average flat and horizontal surfaces of ground and snow. However, the real earth's surface has relief. In order to estimate the influence of topography on the interferometric phase let us assume that the known digital elevation model (DEM) describes the relief. We use the tangent plane and geometric optics approximations when considering the interaction of waves with the surface of snow and soil (see Fig. 13). These planes are the result of roughness averaging of the earth and snow surfaces.

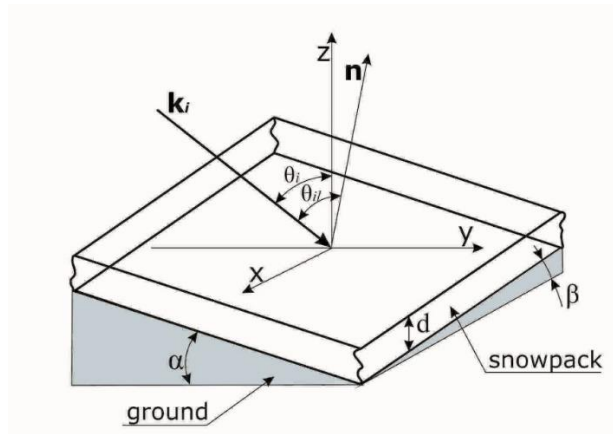


**Figure 3.** The geometry of the wave incidence on the tangent plane, with local slopes.

Electromagnetic wave falls on the snow layer, bounded by the planes "air - snow" and "snow - soil" at a local incidence angle  $\theta_{il}$  and scattered back after refraction in the snow at an angle  $\theta_{il}$  and the passage of the snowpack. The incidence angle (angle of view) is equal to  $\theta_i$  with respect to the vertical axis  $z$ . The wave vector  $\mathbf{k}_i$  is in the  $yz$  plane and the unit wave vector has the form

$$\hat{\mathbf{k}}_i = \sin\theta_i \mathbf{j} - \cos\theta_i \mathbf{k} \quad (\mathbf{j}, \mathbf{k} - \text{unit vectors of the } y \text{ and } z \text{ axes}).$$

The "air – snow" and "snow - soil" planes are parallel to each other and the distance between them vertically (the depth of the snow cover) is equal to  $d$ . The local inclination of these planes is determined from the DEM. The angle  $\alpha$  is measured with respect to the radar coordinate "range" ( $y$ -axis) and angle  $\beta$  with respect to the coordinate "azimuth" ( $x$ -axis). Then the local incidence angle  $\theta_{il}$  at the point with the unit normal  $\hat{\mathbf{n}}$  is determined from equation

$$\cos\theta_{il} = -\hat{\mathbf{k}}_i \cdot \hat{\mathbf{n}} = \frac{\tan\alpha \sin\theta_i + \cos\theta_i}{\sqrt{1 + \tan^2\alpha + \tan^2\beta}}. \quad (9)$$

It follows from (9) that relief inclination in "range" direction most influence on local incidence angle. Let us estimate influence of relief in assumption that  $\beta = 0$ . The local interferometric phase of wave, reflected by soil can be expressed as follows

$$\Phi_{gl} = 2kd \cos\alpha \left( \sqrt{\cos^2(\theta_0 - \alpha) + 1.6\rho + 0.86\rho^3} - \cos(\theta_0 - \alpha) \right) \quad (10)$$

Expression (23) valid both for positive values of  $\alpha$  (front slope) and negative  $\alpha$  values (back slope). Let us estimate the relative changes in the interferometric phase due to the influence of relief with help of the formulas (18) and (23)

$$\delta\Phi_{gl} = \frac{\Phi_{gl} - \Phi_g}{\Phi_g}. \quad (11)$$

Figure 4 shows dependence of  $\delta\Phi$  from the angle  $\alpha$  at different values of  $\theta_i$  and  $\rho$ . These plots prove that the influence of terrain slopes on the relative phase can be quite significant. Relative phase changes reach 40% for steep slopes with

$\alpha$  values of about  $45^\circ$ . However, with gentle slopes, these changes are small. The slope of the relief did not exceed  $1.5^\circ$  changes the interferometric phase do not exceed 2% at these values, which confirms the possibility of using the model of the averaged horizontal surface of the earth in this case.

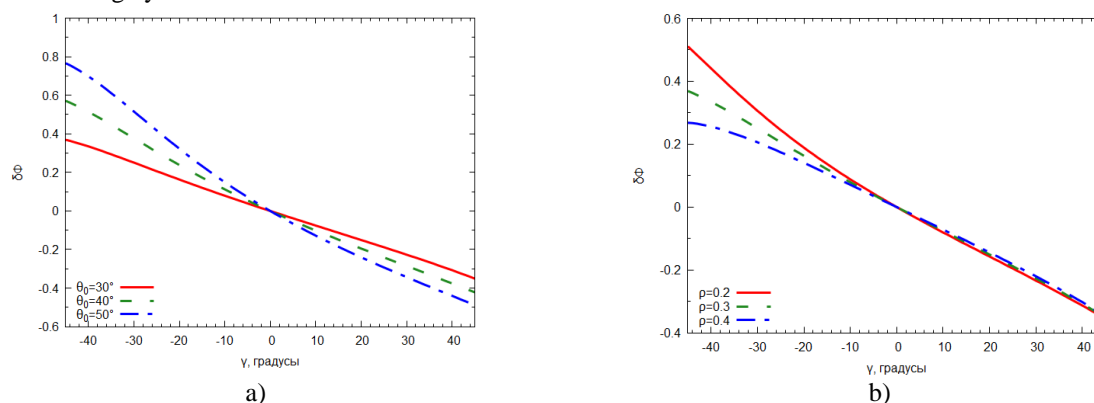


**Figure 4.** Dependences of the interferometric phase relative changes from the angle of inclination of the terrain along the "range" radar coordinate: a) at different  $\theta_0$ ,  $\rho = 0.3 \text{ g/cm}^3$ ; b) at different  $\rho$ ,  $\theta = 30^\circ$ .

### 3 Conclusion

An approximate model is constructed for determining the interferometric phase, which is the phase difference of radar signals in the absence of snow and after snowfall. The model is based on the small perturbation method. An analysis is made of the effect of the backscattering wave on the roughness of the snow cover on the phase of the radar signal. The model is generalized to the general case of backscattering from snow cover on the earth's surface with a relief, and the influence of the slope angles of the relief on the interferometric phase is estimated.

**Acknowledgements.** This work was supported by Russian Foundation for Basic Research (Grant No. 18-05-01051 A).

### References

- [1] Rees W.G. Remote sensing of snow and ice. CRC Press, Taylor & Francis Group, 2006.
- [2] A. Moreira, P. Prats-Iraola, M. Younis, G. Krieger, I. Hajnsek, and K. Papathanassiou. A tutorial on synthetic aperture radar // IEEE Geosci. Remote Sensing Mag. 2013. V. 1. № 1. P. 6–43.
- [3] Hanssen R.F. Radar Interferometry: Data Interpretation and Error Analysis. Dordrecht, Kluwer Academic Publishers. 2001.
- [4] Zakharov A.I., Epov M.I., Mironov V.L., Chymitdorzhiev T.N., Bykov M.E., Seleznev V.S., Emanov A.F., Cherepenin V.A. Earth surface subsidence in the Kuznetsk coal basin caused by manmade and natural seismic activity according to ALOS PALSAR interferometry. // IEEE Journal of Selected Topics in Applied Earth Observations and Remote Sensing. 2013. V. 6. №. 3. P. 1578-1583.
- [5] Beck I., Ludwig R., Bernier M., Strozzi T., Boike, J. Vertical movements of frost mounds in sub-Arctic permafrost regions analyzed using geodetic survey and satellite interferometry. // Earth Surface Dynamics. 2015. V 3. P. 409–421.
- [6] Chimitdorzhiev T.N., Dagurov P.N., Bykov M.E., Dmitriev A.V., Kirbizhekova I.I. Comparison of ALOS PALSAR interferometry and field geodetic leveling for marshy soil thaw/freeze monitoring, case study from the Baikal lake region, Russia // Journal of Applied Remote Sensing. 2016. V. 10. № 1. P. 016006.
- [7] Guneriusson T., Hogda K. A., Johnsen H., Lauknes I. InSAR for estimation of changes in snow water equivalent of dry snow. // IEEE Transactions on Geoscience and Remote Sensing, 2001. V. 39. № 10. P. 2101–2108.
- [8] Rott H., Nagler T., Scheiber R. Snow mass retrieval by means of SAR interferometry. // In 3rd FRINGE workshop. European Space Agency: Earth Observation; [https://earth.esa.int/fringe03/proceedings/papers/46\\_rott.pdf](https://earth.esa.int/fringe03/proceedings/papers/46_rott.pdf).
- [9] Leinss S., Wiesmann A., Lemmetyinen J., Hajnsek I. Snow water equivalent of dry snow measured by differential interferometry. // IEEE J. Sel. Topics Appl. Earth Observ. Remote Sens. 2015. V. 8. №. 8. P. 3773–3790.

- [10] Conde V., G. Nico, P. Mateus, J. Catalão<sup>1</sup>, A. Kontu, M. Gritsevich On the estimation of temporal changes of snow water equivalent by spaceborne SAR interferometry: a new application for the Sentinel-1 mission // *J. Hydrol. Hydromech.* 2019. V. 67. № 1. P. 93–100.
- [11] Dagurov P.N., Chimitdorzhiev T.N., Dmitriev A.V., Dobrynin S.I., Zakharov A.I., Baltukhaev A.K., Bykov M.E., Kirbyzhkova I.I. L-band differential radar interferometry for determining snow cover parameters (in Russian) // *Journal of Radio Electronics.* 2017. No. 5. P. 14. <http://jre.cplire.ru/jre/may17/1/text.pdf>
- [12] Dagurov P.N., Baltukhaev A.K., Dmitriev A.V., Dobrynin S.I., Chimitdorzhiev T.N. Interferometric Model of Radar Sensing of Snow Cover (in Russian). Regional Problems of Remote Sensing of the Earth. Materials V Int. scientific conferences. Siberian Federal University, Institute of Space and Information Technologies. 2018.S. 109-112.
- [13] Ulaby, F.T., R.K. Moore, and A.K. Fung *Microwave Remote Sensing.* Chapter 12. V. 2, Dedham, MA: Artech House, 1982.
- [14] Mätzler C. Microwave permittivity of dry snow // *IEEE Trans. Geosci. Remote Sens.* 1996. V. 34. №. 2. P. 573–581.